
Article:
Agatz, Annika orcid.org/0000-0003-3228-8822 and Brown, Colin David orcid.org/0000-0001-7291-0407 (2017) Introducing the 2-DROPS model for two-dimensional simulation of crop roots and pesticide within the soil-root zone. Science of the Total Environment. pp. 966-975. ISSN: 0048-9697

https://doi.org/10.1016/j.scitotenv.2017.02.076

Introducing the 2-DROPS model for two-dimensional simulation of crop roots and pesticide within the soil-root zone

Annika Agatz [a *]

[a] Environment Department, University of York, Heslington, York, United Kingdom

[*] Corresponding author

annika.agatz@york.ac.uk

+ 44-(0)-1904323118

Colin D. Brown [a]

[a] Environment Department, University of York, Heslington, York, United Kingdom

colin.brown@york.ac.uk

Abstract

Mathematical models of pesticide fate and behaviour in soils have been developed over the last 30 years. Most models simulate fate of pesticides in a 1-dimensional system successfully, supporting a range of applications where the prediction target is either bulk residues in soil or receiving compartments outside of the soil zone. Nevertheless, it has been argued that the 1-dimensional approach is limiting the application of knowledge on pesticide fate under specific pesticide placement strategies, such as seed, furrow and band applications to control pests and weeds.

We report a new model (2-DROPS; 2-Dimensional ROots and Pesticide Simulation) parameterised for maize and we present simulations investigating the impact of pesticide properties (thiamethoxam, chlorpyrifos, clothianidin and tefluthrin), pesticide placement strategies (seed treatment, furrow, band and broadcast applications), and soil properties (two silty clay loam and two loam top soils with either silty clay loam, silt loam, sandy loam or unconsolidated bedrock in the lower horizons) on microscale pesticide distribution in the soil profile.

2-DROPS is to our knowledge the first model that simulates temporally- and spatially-explicit water and pesticide transport in the soil profile under the influence of explicit and stochastic development of root segments. This allows the model to describe microscale movement of pesticide in relation to root segments, and constitutes an important addition relative to existing models. The example runs demonstrate that the pesticide moves locally towards root segments due to water extraction for plant transpiration, that the water holding capacity of the top soil determines pesticide transport towards the soil surface in response to soil evaporation, and that the soil type influences the pesticide distribution zone in all directions. 2-DROPS offers more detailed information on microscale root and pesticide

appearance compared to existing models and provides the possibility to investigate strategies targeting control of pests at the root/soil interface.

Keywords

Zea mays, Pesticide, 2-D, modelling, solute transport

1. Introduction

Mathematical models of pesticide fate and behaviour in soil have been developed over the last 30 years. Applications of these models include use as research tools, support for environmental safety assessments, and design of approaches to manage risks of pesticides (Addiscott and Wagenet, 1985; Kohne et al. 2008). In many cases, models simulate fate of pesticides in soil as a necessary step in quantifying transfer into non-target compartments including groundwater (Boesten, 1994; Brouwer, 1994, Tiktak et al. 2002), surface water (Carsel et al. 1985; Singh and Kanwar, 1995; Jarvis and Larsbo, 2012), crops (Fantke et al. 2013), and air (Bedos et al. 2009). In each instance, it has been sufficient to treat soil as a 1-dimensional system; this system varies in the vertical plane due to variation in boundary interfaces, soil properties, root distribution, pesticide inputs, water fluxes and so on, but variation in the horizontal plane is ignored. Some authors have coupled 1-dimensional models for leaching of pesticides through the soil unsaturated zone with 2- or 3-dimensional simulation of transport in groundwater where lateral transport is the norm (Hantush et al. 2000; Zhu et al. 2013).

Thus the 1-dimensional approach to modelling pesticide fate in soil has been successful in supporting a range of applications where the prediction target is either bulk residues in soil or receiving compartments outside of the soil zone. The 1-dimensional approach addresses the requirements for model parsimony, whereby model descriptions should be as simple as possible whilst fulfilling the prediction need. Nevertheless, it can be argued that the 1-D approach has been a limiting factor on the application of knowledge on pesticide fate. A range of strategies are available to target placement of pesticides into the soil profile, such as seed treatment, in-furrow applications and banding. These strategies afford more targeted placement to control pests and weeds whilst reducing overall inputs of pesticides into the system. However, innovation in this space has been limited because we lack predictive tools

to guide development of placement technologies and to reward technologies by assessing the benefits for risks to the environment.

The literature includes a small number of 2-dimensional models for pesticide fate in soil. The TRANSMIT model (Hutson and Wagenet, 1995) is a multiregion model that comprises multiple iterations of the one-dimensional model LEACHP; transfer of water and chemical between regions allows application to 2-dimensional geometries and non-uniform surface boundary conditions such as drip irrigation or band applications of pesticides. The most frequently applied 2-dimensional model in recent years has been HYDRUS (Šimůnek et al. 2013). HYDRUS is a flexible software package applicable for simulating water, heat and solute movement in 1-, 2- and 3-dimensional porous media. Spatially-explicit solutions of the Richards equation and convection-dispersion equation are supplemented by routines to describe sorption and degradation processes for reactive solutes such as pesticides and the simulation of nonequilibrium transport for two-region/dual porosity systems. HYDRUS-2D was used to evaluate preferential flow processes along a sloping transect at a field site in southern Sweden, demonstrating that a dual permeability description of preferential flow better matched transport of MCPA (2-methyl-4-chlorophenoxyacetic acid) to tile drains than simulations based on mobile/immobile regions or dual porosity (Gärdenäs et al. 2006). More recently, the model has been coupled with measurements of heterogeneity in soil properties across study sites to describe transport of pesticides through field soils (Suarez et al. 2013; Filipović et al. 2014; 2016). Simulation of root growth has been a constraint in HYDRUS with a simplified rooting pattern and definition via input parameters that did not consider the feedback between root growth and conditions in the soil. Recently, these feedbacks with soil water content or temperature have been added to HYDRUS-1D and partially implemented in HYDRUS-2D via an additional root growth module (Hartmann and Šimůnek, 2015). Finally, there has been a limited amount of work to describe fate of soil fumigants in two dimensions,

for example following addition in drip irrigation and including the impacts of two dimensional cultivation beds and differentiated temperature fluctuations across the soil surface (Ha et al. 2009a,b; Luo et al. 2011).

Here we report a new model called 2-DROPS (2-Dimensional ROots and Pesticide Simulation) that describes the spatial and temporal distribution of crop roots and pesticides in the soil-root zone. The model captures spatial differentiation in inputs of precipitation and irrigation to soil (for example due to leaf cover and stem flow), and spatial differentiation in pesticide inputs (for example due to application as seed treatment). Root development is simulated as a spatially explicit and stochastic process within constraints that are specific to the crop, whilst transport of water (modelled according to the capacity approach) and chemical occurs in both vertical and horizontal planes according to hydraulic gradients arising from inputs of water at the surface, soil evaporation and extraction of soil water by the roots. Leaching out of the soil profile is again a spatially explicit process. Overland flow is ignored in the current version of the model but could readily be added as a future development.

2. Model description

2.1. Overview

The aim of this work was to derive a model to predict the temporally- and spatially-explicit transport of water and pesticide in the soil profile with particular focus on the influence of temporally- and spatially-explicit development of the plant root system. 2-DROPS simulates water transport and pesticide fate for a vertical soil profile of 76 * 100 cm (x- and y-axes) and 1 cm depth (z-axis) with each patch/grid representing 1 cm^3. These dimensions were selected to represent the root zone of a single plant in a commercial maize field; the spatial dimensions could be modified to describe crops with different rooting

systems. The model is implemented in NetLogo 5.0.5 (Wilensky 1999) and runs at a daily resolution from the beginning of a year (Julian day 1) until a day specified by the user. Irrigation can be implemented by the user, which then alters the above ground plant development and initiates an irrigation schedule that is dependent on climate and soil type. Whilst water can move in either direction horizontally and vertically, water leaching from the base of the soil profile is considered lost from the system. The soil can be divided into up to four horizons with differing soil characteristics. A schematic flow chart illustrating the order of processes incorporated in the model is presented in Figure 1.

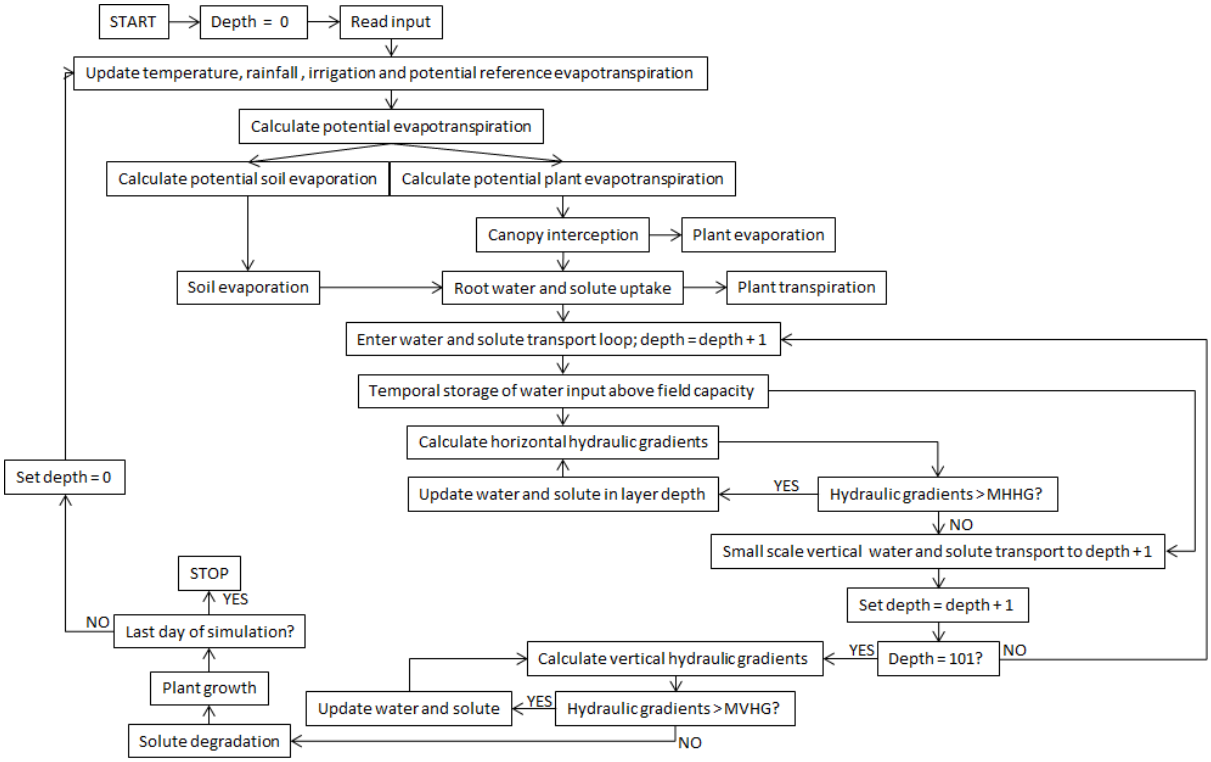

Figure 1: Flow chart for the organisation of model processes.

Inputs for 2-DROPS in addition to those described in the detailed model description (Section 2.2.) and the Appendix (Nomenclature) are the soil horizon boundaries, whether

irrigation occurs, the planting and application day, and the application type and application rate.

2.2. Details

2.2.1. Evapotranspiration

The general formula to calculate the crop specific evapotranspiration $\mathbf{ET_a}$ from the reference evapotranspiration and two crop-specific coefficients is:

$$ET_a = K_o * K_c * ET_r$$

where $\mathbf{K_c}$ is the crop coefficient, $\mathbf{K_o}$ is the water stress coefficient and $\mathbf{ET_r}$ is the daily reference evapotranspiration (Allen et al. 1998). The latter can either be direct input data from a weather

D_r) / (1- station or can be calculated using weather data and for example the FAO Penman-Monteith method.

The crop coefficient $\mathbf{K_c}$ for maize is given as a function of time after plant emergence $\mathbf{T_{spe}}$ using the duration of different plant growth stages and the corresponding crop coefficients given in the literature (Allen et al. 1998):

$K_c = 0.3$ for $T_{spe} < 30$

$K_c = 0.3 + ((T_{spe} - 30) * 0.0225)$ for $T_{spe} > 30 < 70$

$K_c = 1.2$ for $T_{spe} >70 < 120$

$K_c = 1.2 – ((T_{spe} - 120) * 0.012)$ for $T_{spe} > 120$

The water stress coefficient $\mathbf{K_o}$ is calculated taking into account the total of root available water **TAW**, the root depletion factor $\mathbf{D_r}$ and a fraction **p** of **TAW** that a plant can extract from the root zone without water stress:

$$K_o = (TAW – p) * TAW)$$

$$TAW = \Sigma (C_{fc} – C_{wp})_R + \Sigma ((C_{fc} – C_{wp})_{RN})$$

$$D_r = \Sigma\,(C_{fc} - C)_R + \Sigma\,((C_{fc} - C)_{RN})$$

The total root available water **TAW** in the soil profile is calculated as the sum of the difference between the water content at field capacity $\mathbf{C_{fc}}$ and that at the wilting point $\mathbf{C_{wp}}$ of each grid cell containing a root segment (subscript $_{\mathbf{R}}$) and the eight direct neighbouring grid cells (subscript $_{\mathbf{RN}}$) (this set of nine cells is defined as the water extraction zone for a root segment). The zone for water extraction by root segments was specified as an approximation according to McCully (1999); it was shown that fine roots of maize (defined as branch roots with a diameter of less than 0.8 mm) that are the major source of water uptake into the plant, are in 98% of cases 3 cm long or less. Cells that are part of the water extraction zone for more than one root segment only contribute once to the calculation of the water stress coefficient. This calculation differs from the usual procedure in one-dimensional models of calculating the total root available water, where a root fraction parameter is used to scale available water according to the amount of root material (e.g. SPIDER (Renaud et al. 2008)). Here, the root fraction parameter is replaced by information on the appearance of root material in time and space derived from the temporally- and spatially-explicit model of the maize root system (see section on *Crop processes* for details).

The root depletion factor $\mathbf{D_r}$ is given as the sum of the differences between the water content at field capacity $\mathbf{C_{fc}}$ for cells in the water extraction zone of each root segment.

Our model assumes that there is no plant material on the field prior to planting of maize. Thus there is no adjustment of the water stress coefficient prior to planting (i.e., $\mathbf{K_o} = 1$) and the crop coefficient is set to the crop coefficient at the initial growth stage of maize (i.e., $\mathbf{K_c} = 0.3$) assuming that the soil surface is mostly bare (Allen 2003).

Once derived, the crop specific evapotranspiration is used to determine the potential soil evaporation $\mathbf{E_s}$ and the potential plant evapotranspiration $\mathbf{E_c}$ (Belmans et al. 1982).

$$E_s = ET_a * e^{(-0.6\ LAI)}$$

$$E_c = ET_a - E_s$$

The user defines a soil evaporation depth **SED** which determines to what depth the grid cells with a water content above the wilting point contribute to soil evaporation. If the available water content of the cells **C** (water stored between the wilting point $\mathbf{C_{wp}}$ and the field capacity $\mathbf{C_{fc}}$) is larger than the potential soil evaporation $\mathbf{E_s}$ divided by the number of grid cells above the soil evaporation depth **SED** along the entire width of the 2-dimensional area **X** to be covered $\mathbf{E_{s(i)}}$ then the water content **C** is updated extracting $\mathbf{E_{s(i)}}$ of each grid cell in the soil evaporation zone. If the potential soil evaporation $\mathbf{E_s}$ is not satisfied (i.e. at least one grid cell in the soil evaporation zone is not able to satisfy its $\mathbf{E_{s(i)}}$) then the water content of that cell equals the water content at the wilting point and the remaining soil evaporation requirement is addressed in a further iteration of the soil evaporation process; this is achieved by cells in the evaporation zone with water contents above wilting point sharing equally the soil evaporation that remains to be satisfied. This process is repeated until the whole soil evaporation is satisfied (i.e., potential soil evaporation = actual soil evaporation) or to a maximum of 500 iterations.

2.2.2. Irrigation

Irrigation is optional, and when chosen alters the above ground plant development and initiates an irrigation schedule that depends on accumulated deficit **AD** and varies with climate category and soil type. The irrigation schedule is implemented according to the estimation method described by the Food and Agriculture Organisation of the United Nations (Brouwer and Prins 1989) adjusted to the actual accumulated deficit **AD** in the soil profile (i.e. the difference between the maximum water content and the actual water content of all cells; $AD = \Sigma (C_{fc} - C_{wp}) - \Sigma C$). The estimation method (Brouwer and Prins 1989) for the irrigation schedule determines how often and how much water is added to the maize field

depending on the soil category (sandy, loamy or clayey) and the climate category (1, 2, or 3; which represent situations where the reference crop evapotranspiration is 4-5, 6-7 and 8-9 mm/d, respectively). Both, the climate category and the soil category can be chosen by the user from a predefined set. This schedule is adjusted to account for actual accumulated deficit **AD**; which initiates irrigation according to the estimated schedule on demand subsequent to root emergence. Demand is defined as the time point when the accumulated deficit **AD** is greater than the net irrigation depth **I** and instantly initiates irrigation.

2.2.3. Crop processes

Crop processes included in 2-DROPS are the temporally- and spatially- explicit root model, the temporally-explicit model of shoot development, uptake of water and pesticide by roots, interception of rainfall and irrigation by the canopy, and evaporation from the canopy.

The temporally- and spatially-explicit appearance of root segments is simulated according to the sub-model of root-growth implemented in the POPP-Corn model (Agatz et al. 2016) where maize root development is explicitly simulated for maize root nodes 1–7. Root development occurs in two parts. The first part is the time dependent, spatially restricted (but within these boundaries stochastic) appearance of new root segments that are not directly linked to another, whilst the second part describes the actual growth of root biomass over time.

Above ground plant development is expressed as the leaf area index **LAI** and the fraction of the surface covered by crop canopy **FCC** which is derived from the **LAI.** The literature suggests that the leaf area index **LAI** for maize increases faster over time for plants in irrigated (subscript $_{\mathbf{I}}$) than in solely rain-fed (subscript $_{\mathbf{RF}}$) fields (Nguy-Robertson et al. 2012). Data from the literature (Nguy-Robertson et al. 2012) were fitted with a three parameter log normal peak function in SigmaPlot (version 13.0, Systat Software, San Jose,

CA) to derive the following equations which describe time-dependence of the leaf area index for irrigated and rain-fed maize plants, respectively.

$$LAI_I = a_I * \exp(-0.5 * (\ln(T_{spe} / c_I) / b_I) \wedge 2) / T_{spe}$$

$$LAI_{RF} = a_{RF} * \exp(-0.5 * (\ln(T_{spe} / c_{RF}) / b_{RF}) \wedge 2) / T_{spe}$$

Parameter values for a, b and c are provided in Table 1 and a graphical illustration of the fits is provided in Figure 2, left. Literature data (Andrieu et al. 1997) were fitted with an exponential rise to maximum curve (Simple Exponent, 2 Parameter) in SigmaPlot to derive a correlation between **LAI** and **FCC** for maize. A graphical illustration of the fits is provided in Figure 2, right.

$$FCC = 0.9622 * (1 - 0.6756^{LAI})$$

Table 1**:** Parameter values for calculation of the leaf area index **LAI** of maize in irrigated ($_I$) or rain-fed ($_{RF}$) fields.

	A	B	C
Irrigated	440.9	0.440	75.56
Rain fed	307.7	0.424	76.29

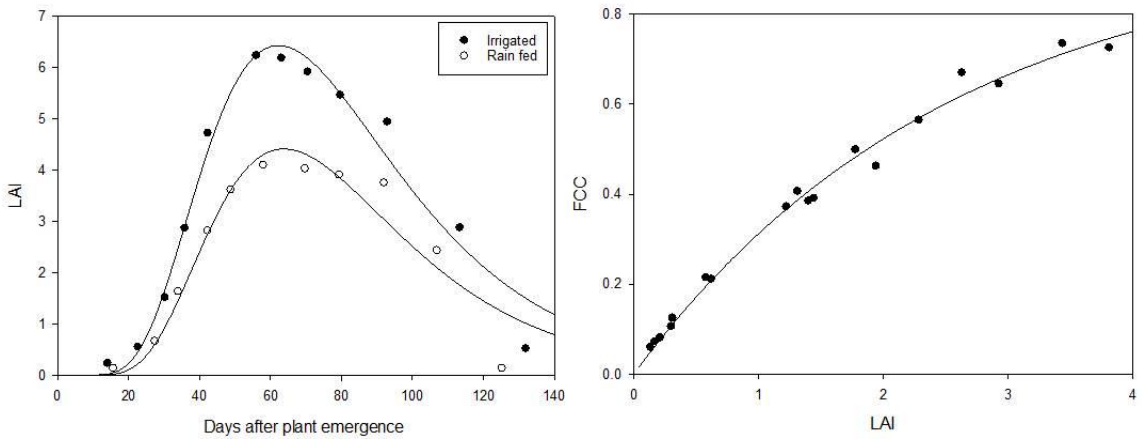

Figure 2: Leaf area index (LAI) over time for irrigated and rain fed maize (left), and fraction of crop coverage (FCC) over LAI (right). The lines indicate the functions fitted to literature data (left: Nguy-Robertson et al. 2012; right Andrieu et al. 1997).

As a first approximation, a linear increase of the water storage capacity of the canopy $\mathbf{S_c}$ by 0.2 mm per unit **LAI** is assumed (Renaud et al. 2008) and the portion of the water falling on the crop $\mathbf{R_c}$ is calculated using the daily rainfall **R**, the amount of water added through irrigation **I** and the fraction of the surface covered by crop canopy **FCC** ($R_c = R + I * FCC$). The water stored on the crop $\mathbf{W_{can}}$ for each day is calculated as a balance between how much water is still stored on the canopy, the rain and irrigation falling onto the canopy and the amount of water evaporating from the canopy; $\mathbf{W_{can}}$ cannot exceed the water storage capacity of that particular day. The difference between the portion of the rain and irrigation falling on the crop $\mathbf{R_c}$ and the water stored on the crop $\mathbf{W_{can}}$ is used to determine the amount of water that reaches the ground by throughfall **TF**.

$TF = 0$ if $R_c < S_c - W_{can}$

$TF = R_c - S_c - W_{can}$ if $R_c > S_c - W_{can}$

Throughfall **TF** comprises a proportion dripping through the canopy and a proportion entering the soil via stem flow **SF** into the stem flow area **SFA**. Stem flow depends on multi-dimensional canopy development and its intensity and exact horizontal input to the top soil layer depends on crop type, growth stage, row spacing and rainfall intensity. Thus, literature information varies considerably. For example, Norman and Campbell (1983) showed for maize that 25-60% of all rainfall intercepted by the canopy reached the soil as stem flow Paltineanu and Starr (2000) demonstrated that the ratio of stem flow to throughfall depended on rainfall intensity and plant growth stage and can be as small as 0.8 or exceed 3. As an approximation, we direct 50% (i.e. SF = 0.5) of the throughfall to enter the soil at the cell where the seed was planted and the three neighbouring cells in both directions (i.e. SFA = 7 cm) for all rainfall and irrigation events. The remaining 50% of the throughfall is distributed equally across the soil surface below the canopy but outside the stem-flow area. As rainfall and irrigation is treated equally regarding infiltration at the soil surface, our approach is only

valid for sprinkler irrigation systems. Soil not covered by canopy receives the full amount of rain and/or irrigation. The area of the soil covered by canopy but not associated with the stem flow area generally changes with plant growth. As an approximation we use the fraction of the surface covered by crop canopy **FCC** to determine which cells of the soil surface are covered with plant material; assuming coverage from the centre of the grid equally towards both sides.

To satisfy the crop specific evapotranspiration $\mathbf{ET_a}$ water can evaporate from the canopy (wet canopy evaporation $\mathbf{E_{cw}}$), transpire following root uptake of water ($\mathbf{E_r}$ potential root water uptake), or can occur from a combination of both ($ET_a = E_{cw} + E_r$). Wet canopy evaporation $\mathbf{E_{cw}}$ only takes place when the canopy has stored water, at which point evaporation occurs according to a transformed plant evapotranspiration rate until the water stored in the canopy is depleted ($E_{cw} = ET_a * C_f$), where $\mathbf{C_f}$ is an empirical correction factor accounting for enhanced evaporation from a wet canopy (≥ 1) which can be adjusted by the user. If the water stored in the canopy $\mathbf{W_{can}}$ is greater than the wet canopy evaporation $\mathbf{E_{cw}}$, then the water stored in the canopy $\mathbf{W_{can}}$ is updated by extracting $\mathbf{E_{cw}}$. If the canopy is depleted ($W_{can} = 0$) but $\mathbf{ET_a}$ is not satisfied, the remaining water requirement is extracted from the soil via root water uptake $\mathbf{E_r}$; evaporation in this case occurs according to the $\mathbf{ET_a}$ rather than $\mathbf{E_{cw}}$. When a potential root water uptake $\mathbf{E_r}$ exists, this demand is satisfied by all cells in the soil profile that contain root segments. First a cell specific root water uptake $\mathbf{E_{r(i)}}$ is calculated dividing by $\mathbf{E_r}$ by the number of root segments $\mathbf{N_{rs}}$ present in the profile. If the available water content of a cell **C** containing a root segment multiplied by the fraction of available water that a plant can extract from the root zone without water stress **p** is higher than $\mathbf{E_{r(i)}}$, then the water content **C** of a cell is updated extracting $\mathbf{E_{r(i)}}$ from the actual water content. In this case, the actual root water uptake of that root segment $\mathbf{AE_{r(i)}}$ equals its potential root water uptake $\mathbf{E_{r(i)}}$. If the root water uptake $\mathbf{E_r}$ is not satisfied by the cells

containing roots (e.g. at least one root segment has an $\mathbf{AE_{r(i)}} < \mathbf{E_{r(i)}}$) then the actual water content **C** of the cell(s) with root segment(s) that have an $\mathbf{AE_{r(i)}} < \mathbf{E_{r(i)}}$ is readjusted by extracting water from its eight neighbouring cells (i.e. the zone for water extraction by root segments, illustrated in Figure 3).

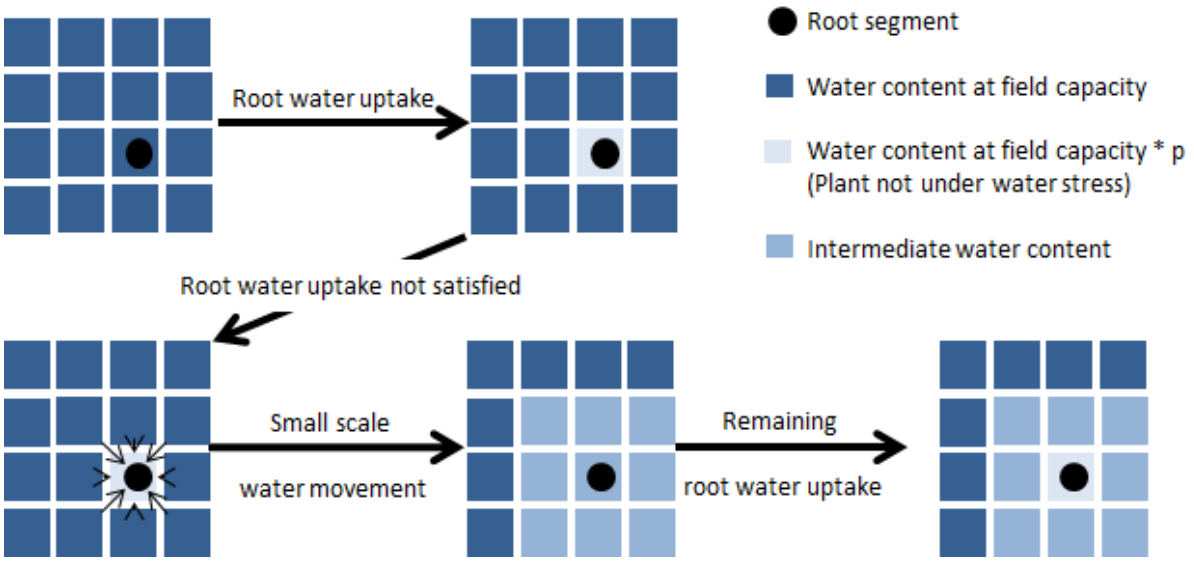

Figure 3: Schematic illustration of the zone for water extraction by root segments under drought conditions for cells with root segments.

If this readjustment is not sufficient for the cell with the root segment to satisfy $\mathbf{E_{r(i)}}$ then the cell containing the root increases its $\mathbf{AE_{r(i)}}$ by the amount of water gained from its neighbouring cells; a new iteration of the procedure is then initiated to satisfy the root water uptake $\mathbf{E_r}$ and repeated until either $\mathbf{E_r}$ is satisfied or 500 iterations have passed. 500 iterations was chosen as a limit for the root water uptake procedure to allow sufficient extraction of water from neighbouring cells to satisfy $\mathbf{E_r}$ without prohibitive demands on computing time; the maximum inaccuracy in the total water balance imposed by this limit was 0.005%.

2.2.4. Transport of water

Movement of water is modelled using the soil capacity approach and occurs subsequent to soil evaporation each day. The capacity approach uses soil water holding capacity to drive transport of water (e.g. Klein 1991) and was selected over a classical simulation of water movement in unsaturated soil based on the Richards equation (e.g. Šimůnek et al. 2013) as a compromise between accuracy of simulation, ease of parameterisation and computational time.

Overall, water movement (excluding the minimal movement to satisfy canopy transpiration) occurs according to the following pattern. First rain/irrigation and/or throughfall enter the uppermost 1-cm layer of the soil profile. If the amount of water entering a cell in the upper layer exceeds the field capacity of the cell, then the remaining water is deposited in a temporary storage followed by horizontal movement within the first layer. Should the horizontal movement provoke a cell with water in temporary storage to have a water content below field capacity, then the water content of the cell is returned to a maximum of its field capacity using water from the temporary storage. When horizontal movement in the upper layer is complete (a full description of boundary conditions is given below), the remaining water in the temporary storage of each cell is vertically transported to the next layer (small-scale vertical transport) which then processes the horizontal movement. Only if this procedure (horizontal movement within layers and small scale vertical transport) is completed over the entire depth of the soil profile will any remaining water above field capacity of individual cells in the bottom layer leach out of the base of the soil profile.

Water transport (excluding the minimal movement to satisfy canopy transpiration and small-scale vertical transport) is controlled by user defined maximum hydraulic gradients, a mechanism adapted from the implementation made by Garratt and Wilkins (1999) to simulate horizontal water movement in their 2D-Varleach model. In their model, a permitted maximum hydraulic gradient **MHG** was used to move water horizontally when a sufficiently

steep hydraulic gradient existed within the soil layer. The specific hydraulic gradient **HG** was calculated for all pairs of neighbouring cells (i.e. cell 1 & 2, cell 2 & 3, …) by dividing the larger and smaller water content of the two adjacent cells; for those pairs with HG > MHG, Garratt and Wilkins (1999) allowed water to flow from the cell with the larger water content to the cell with the smaller water content until the water contents were equalised.

We use a variation of the maximum hydraulic gradient method for both the horizontal water movement and vertical transfer of water below field capacity (e.g. in response to water extraction by roots or via soil evaporation). Thus, our model has a permitted maximum horizontal hydraulic gradient **MHHG** which is compared to the horizontal hydraulic gradient **HHG** from pairs of horizontally neighbouring cells (i.e. cell 1 & 2, cell 2 & 3, …) and a permitted maximum vertical hydraulic gradient **MVHG** which is compared to the vertical hydraulic gradient **VHG** from pairs of vertically neighbouring cells (i.e. cell 1in layer 1& cell 1in layer 2, cell 1in layer 2 & cell 1in layer 3…). **MHHG** and **MVHG** are independent of each other and both are user defined.

In contrast to Garratt and Wilkins (1999), we calculate the hydraulic gradients (**HHG** and **VHG**) between pairs of cells using only the mobile fraction of the water in each cell rather than the whole water content. This change in approach allows the procedure of water movement to be consistent (in terms of how much water is transferred in each step) across different soils (i.e. differing field capacities and wilting points) with the same hydraulic gradient. To avoid dividing by zero in the calculation of hydraulic gradients, we assume that cells at wilting point have a negligibly small amount of movable water (0.0001 mm).

The horizontal movement in each layer is executed for all layers according to the **MHHG** as the rain and/or throughfall makes its way down the soil profile. This downwards movement of water entering the system (small scale vertical transport) is only controlled by water stored in the temporary storage and not by **MVHG.** The large scale vertical movement

according to the **MVHG** is only initiated when the horizontal movement in layer 100 is completed and this layer has released any water held in temporary storage as leachate from the base of the soil profile. A substantial difference to the implementation made by Garratt and Wilkins (1999) is that we only allow 1% of the difference in available water content between adjacent cells to move at each iteration rather than equalising the water content of cells in a pair when **HG** is higher than the permitted maximum hydraulic gradient (**MHHG** or **MVHG**). Then the check for hydraulic gradients is repeated and a further 1% of the difference in available water between adjacent cells is moved until the hydraulic gradient between pairs of cells is below the permitted maximum hydraulic gradient. This variation allows the water contents to be adjusted iteratively until the difference in water contents is just below the maximum hydraulic gradient rather than allowing a total equalisation between adjacent cells. Additionally, we allow the left and right border of our grid (i.e. cell 76 & cell 1) to follow the rules for water transport according to the **MHHG**, which ultimately allows our grid to represent a single plant in a maize field with a row spacing of 76 cm.

2.2.5. Chemical processes

Four types of application to soil are possible, namely seed treatment, in-furrow application, banded application, and broadcast application. For seed treatment, the compound is entirely positioned in the grid cell of the seed (the default position is the central cell of the horizontal grid and at 5-cm depth). For furrow application, the default is that the compound is distributed equally between the cell containing the seed and its eight neighbouring cells. If a band application is chosen, the user has to define the width of the band which is centred on the cell containing the seed; the applied chemical is then equally distributed within the area above the seed that has the user-defined width. Broadcast application is equally distributed into the upper 1 cm of soil across the full width of the soil profile. All application types

assume that the additional water that enters the soil during the application process is negligible for the soil water balance (typical rates of water addition for broadcast applications are in the range 0.01 to 0.04 mm).

Degradation of the pesticide is simulated using the degradation rate constant **μ** accounting for effects on rate of degradation of temporally- and spatially-explicit variation in soil temperature and water content. The degradation rate constant **μ** is calculated using the reference degradation rate constant μ_r, a factor accounting for the dependence on water content **Fw**, a factor accounting for the dependence on temperature **Ft** and a factor to adjust for changes in degradation with depth from the soil surface **DDF**. As both water content and soil temperature are simulated as spatially explicit, each cell has an individual **μ** at any point in time which is updated whenever the water content and/or temperature changes.

$$\mu = \mu_r * Fw * Ft * DDF$$

The reference degradation rate constant μ_r is calculated using the half-life of the compound in soil DT_{50s} ($\mu_r = 0.693 / DT_{50s}$). The soil moisture response function and the soil temperature response function used in the MACRO model (Jarvis et al. 1997) were applied to derive **Fw** and **Ft** as follows**:**

$$Fw = (C_{fc} / C_{wp})^{0.5}$$

$$Ft = \exp(0.08 (T - T_{ref})) \quad \text{for } T > 5$$

$$Ft = T / 5 * \exp(0.08 * (5 - T_{ref})) \quad \text{for } 5 > T > 0$$

$$Ft = 0 \quad \text{for } T < 0$$

where **T** is the daily average temperature in the grid cell and T_{ref} is the temperature at which the reference degradation rate constant μ_r was measured. The correction factor for depth dependency of degradation **DDF**, which represents the reduction of biological degradation with soil depth, has been implemented in accordance with the description in the FOCUS groundwater scenarios (FOCUS 2000). Here we fixed **DDF** to 1 for soil layers up to

30 cm depth, 0.5 for soil layers at 30-60 cm depth, and 0.3 for soil layers deeper than 60 cm. The resulting grid cell-specific degradation rate constant **μ** is then used to update the total amount of the compound in the cell **TC** according to single first-order kinetics to degrade the compound ($TC_{(t)} = TC_{(t-1)} * e^{-\mu}$).

Whenever water is transported from one cell to the next, the compound associated with the moving water moves simultaneously. Once inter-cell movement of water and pesticide has occurred, cells-specific sorption of pesticide is recalculated before any further movement of water and pesticide is allowed. Subsequently distribution of the pesticide between the mobile and stationary soil water occurs whereby all water fractions contain the same pesticide concentration. Sorption of pesticide to soil is simulated as a linear and instantaneous process with the distribution coefficient $\mathbf{K_d}$ for each cell calculated using the organic carbon partition coefficient of the pesticide $\mathbf{K_{oc}}$ (PPDB Database 2013) multiplied by the fraction of organic carbon in each soil layer $\mathbf{F_{oc}}$. The total amount of compound in an individual cell **TC** is then used to calculate the total amount of the compound (i) in the water phase of that cell $\mathbf{TC_w}$ ($TC_w = TC / (kd * (B/C) + 1)$), (ii) sorbed to soil $\mathbf{TC_s}$ ($TC_s = TC - TC_w$), (iii) present in the immobile water **TCws** ($TC_{ws} = (TC_w / C) * C_{wp}$), and (iv) present in the mobile water $\mathbf{TC_{wm}}$ ($TC_{wm} = TC_w - TC_{ws}$).

Whenever water is taken up by the root, the mobile fraction of the compound $\mathbf{TC_{wm}}$ is also subjected to root uptake. Root uptake is implemented according to the description in MACRO (Jarvis et al. 1997), where uptake is a function of the root uptake factor **RUF** and the water taken up by the root segment $\mathbf{RAE_{r(i)}}$. This determines the amount of the compound taken up by the roots $\mathbf{TC_r}$**.** The root uptake factor **RUF** is a user defined input parameter between 0 and 1(here, pre-set to 0.5).

$$TC_r = RUF * TC_{wm} * RAE_{r(i)}$$

$$RAE_{r(i)} = (AE_{r(i)} / C - C_{wp})$$

3. Model demonstration

Example runs were undertaken to illustrate the performance of 2-DROPS under a range of input parameters, with the prediction target being the distribution of water and pesticide in the soil profile 60 days after simultaneous sowing of a maize crop and treatment with pesticide. The runs were a) a single pesticide (thiamethoxam, Table 2) applied using the four possible application types (seed treatment, furrow, band and broadcast application); b) four pesticides with contrasting physico-chemical properties all furrow applied (Table 2); c) thiamethoxam furrow applied to four different soils (Table 3); and d) thiamethoxam furrow applied to a single soil type for simulations with a range in values for the maximum hydraulic gradients (horizontal and vertical).

Simulations for a) and b) were conducted for one soil type (Table 3 Urbana). Details for the different soils used are provided in Table 3. These soils represent a soil at the University of Illinois research and education centre in Urbana (Illinois, USA) and three soil types from the FOCUS modelling scenarios (FOCUS 2000). Weather data for the year 2011 were derived from Bondville, Central Illinois, USA (Illinois Climate Network 2016), a weather station close to the research and education centre in Urbana. The soil evaporation depth **SED** was set at 10 cm as the literature suggests that surface evaporation is limited to 5 to 10 cm in maize fields in Illinois (Hollinger and Angel 2009). Both, weather data and soil evaporation depth were used for all simulations and with all soil types considered.

Planting and application occurred at the same day (Julian day 130) and application rates were fixed to 1 mg a.s./seed or 1 mg a.s./m row of the compounds listed in Table 2 independent of the pesticide or application type. The water content of each grid cell at the start of the simulation was set equal to that at field capacity.

Table 2: Properties derived from the literature (PPDB Database 2013) for the four pesticides simulated in Figure 4.

Compound	DT_{50} soil (20°C)[d]	K_{OC} [L/Kg]	Wsol [mg/L]
Thiamethoxam	121	56.2	4100
Clothianidin	545	123	340
Chlorpyrifos	76	8151	1.5
Tefluthrin	37	112900	0.016

Table 3: Soil properties for the soils at the University of Illinois research and education centre in Urbana, and three soils from the FOCUS scenarios (FOCUS 2000).

Soil	Horizon	Depth (cm)	Texture class	Field capacity (cm^3/cm^3)	Wilting point (cm^3/cm^3)	Bulk density (g/cm^3)	Organic carbon (%)
Urbana	A	0-36	Silty clay loam	0.440	0.220	1.20	3.20
	B	360-100	Silty clay loam	0.430	0.200	1.32	0.70
Piacenza	Ap	0-40	Loam	0.341	0.113	1.30	1.26
	Bw	40-80	Loam	0.317	0.065	1.35	0.47
	2C	80-100	Silt loam	0.163	0.022	1.40	0.00
Okehampton	A	0-25	Loam	0.358	0.148	1.28	2.20
	Bw1	25-55	Loam	0.340	0.125	1.34	0.70
	BC	55-85	Sandy loam	0.290	0.090	1.42	0.40
	C	85-100	Sandy loam	0.228	0.050	1.47	0.10
Châteaudun	Ap	0-25	Silty clay loam	0.374	0.253	1.30	1.39
	B1	25-50	Silty clay loam	0.374	0.235	1.41	0.93
	B2	50-60	Silt loam	0.372	0.235	1.41	0.70
	IIC1	60-100	Limestone	0.386	0.185	1.37	0.30

4. Results and discussion

The example runs demonstrate the applicability of the model to account for compound-, soil-, and application-specific differences in the two-dimensional water and pesticide distribution in the soil profile. Overall, the example runs show the stochastic distribution of root segments (Figures 4 - 7). While the distribution of the root system in the soil profile is very similar, the exact appearance of single root segments varies with each model run, but produces a similar picture for the water content across the soil profile. At the profile scale, the water content of the soil increases with increasing distance from the centre of the root system, which is also the case for each single root segment. Figure 7 illustrates that this water

distribution around the roots depends strongly on the maximum hydraulic gradients for both vertical and horizontal water movement. The gradient of water distribution around the root segments in all directions is similar when the maximum hydraulic gradients have the same value and the zone of soil affected by water redistribution around each root segment decreases with increasing gradients (Figure 7 A-D). Choosing one of the gradient values to be low and the other to be high (Figure 7 E and F) shows that the maximum hydraulic gradient for horizontal water movement has a greater impact on the water gradient towards the root segments than the maximum hydraulic gradient for vertical water movement. This is because the horizontal water movement precedes the vertical movement in our model structure. Using the maximum hydraulic gradient method might be an intuitive and simple way of handling water dynamics but we are not aware of any attempts to validate the method or of any empirical data available to do so. This is certainly a vital part of future work, as in the current version it is unclear what value to choose for the gradients and how much they differ between soils. One would expect the gradients to differ between soil types and associated differences in porosity.

Figure 5 demonstrates a strong influence of physico-chemical properties of the pesticide (Table 2) on compound distribution 60 days after application. Overall, the area of the soil profile containing pesticide increases with decreasing soil organic carbon-water partition coefficient and increasing half-life. The example runs also illustrate that the pesticide moves with the water horizontally and vertically, and particularly towards root segments due to the water uptake of roots. This ability to account for microscale movement of pesticide in relation to root segments is an important addition relative to existing models; it offers the possibility to use the model to investigate strategies targeting control of pests at the root/soil interface.

Whilst pesticide distribution varies with soil type (Figure 6), soil characteristics seem to have a smaller influence on the distribution of pesticide across the soil profile than physico-chemical properties of the pesticide or application type (Figure 6). Once a validated estimation is available of how the hydraulic gradients vary with soil types, the relative contribution of soil characteristics in determining pesticide distribution might change. Despite this shortcoming, the example runs show that the pesticide distribution differs with soil type. Here, the overall area containing thiamethoxam increases from Urbana to Châteaudun via Okehampton and Piacenza. The A horizon of Châteaudun soil has a relatively small difference in water contents at field capacity and wilting point (i.e. 0.12) in comparison to the other three soils (0.22 - 0.23) and this resulted in greater upwards movement of the pesticide (Figure 6D) alongside water movement from deeper layers to fulfil soil evaporative demand. The influence of soil characteristics on pesticide distribution indicates that the efficacy of a pesticide against the same pest under the same pest pressure with the same application type and application rate differs for different soils.

Currently the model is not publicly available. The next stage in model development will be thorough testing through comparison to experimental data and other 2-dimensional fate models. We believe the model addresses the requirements for model parsimony, whilst fulfilling the prediction needs to allow research into different pesticide placement strategies in the future. 2-DROPS is to our knowledge the first two-dimensional fate prediction tool that considers precise root appearance in the soil profile.

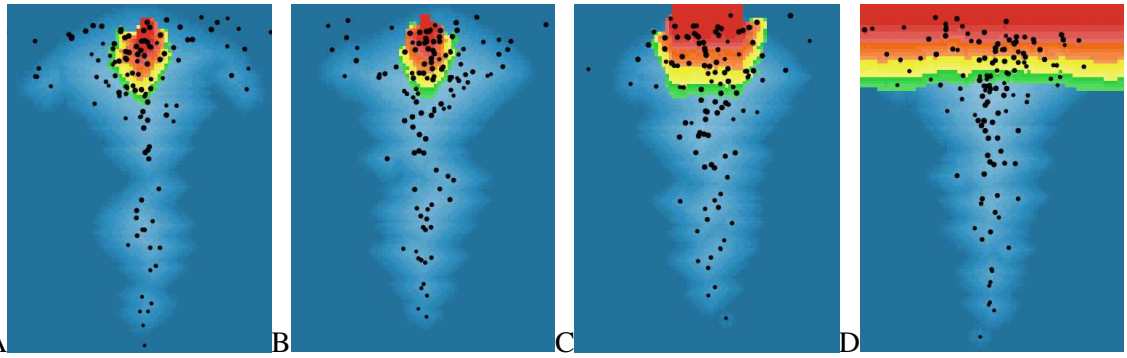

Figure 4: Simulated distribution of water and thiamethoxam (a.i.) in a soil profile 60 days after four differing applications at sowing time; **A** seed, **B** furrow, **C** band, and **D** broadcast. **Blue** (dark to pale): Water content between field capacity and wilting point. **Red-Orange-Yellow-Green**: Compound concentration (ppm) high to low. **Black dots** indicate root segments. Simulations were conducted with maximum hydraulic gradients (vertical and horizontal) of 1.05.

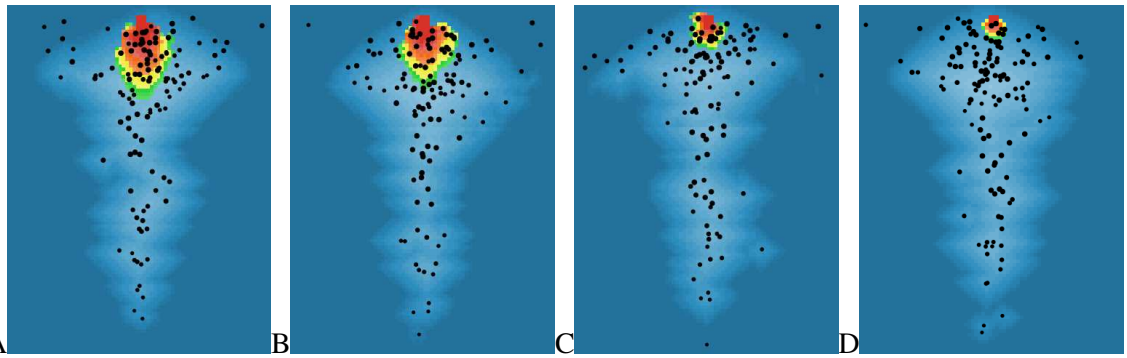

Figure 5: Simulated distribution of water and pesticide in a soil profile 60 days after furrow application; **A** thiamethoxam**, B** clothianidin**, C** chlorpyrifos**, D** teflutrin**. Blue** (dark to pale): Water content between field capacity and wilting point. **Red-Orange-Yellow-Green**: Compound concentration (ppm) high to low. **Black dots** indicate root segments. Simulations were conducted with maximum hydraulic gradients (vertical and horizontal) of 1.05.

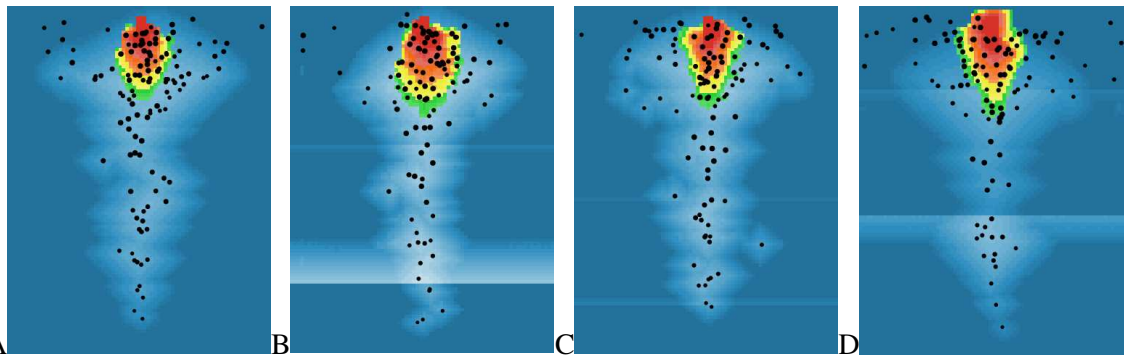

Figure 6: Simulated distribution of water and thiamethoxam (a.i.) in a soil profile 60 days after furrow applications at sowing time for four different soils; **A** Urbana, **B** Piacenza, **C** Okehampton, and **D** Châteaudun. **Blue** (dark to pale): Water content between field capacity and wilting point. **Red-Orange-Yellow-Green**: Compound concentration (ppm) high to low. **Black dots** indicate root segments. Simulations were conducted with maximum hydraulic gradients (vertical and horizontal) of 1.05.

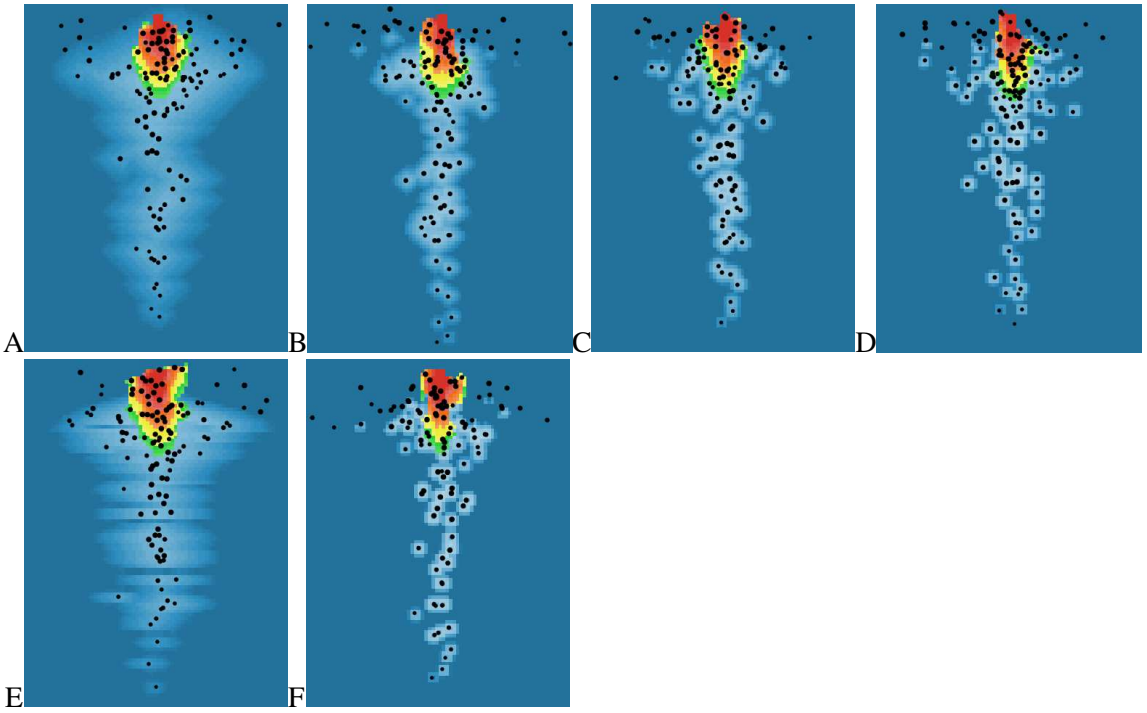

Figure 7: Simulated distribution of water and thiamethoxam (a.i.) in a soil profile 60 days after furrow applications at sowing time for different combinations of the maximum hydraulic gradients for horizontal and vertical water and pesticide flow, respectively; **A** 1.05 and 1.05, **B** 1.2 and 1.2, **C** 1.4 and 1.4, **D** 1.8 and 1.8, **E** 1.05 and 1.8, **F** 1.8 and 1.05. **Blue** (dark to pale): Water content between field capacity and wilting point. **Red-Orange-Yellow-Green**: Compound concentration (ppm) high to low. **Black dots** indicate root segments.

Appendix: Nomenclature

Input data

ET_r	reference evapotranspiration [mm/d]
I	amount of water added through irrigation [mm]
R	daily rainfall [mm/d]

Input parameter

Soil specific

B	bulk density [-]
C_{fc}	water content at field capacity [m^3/m^3]
C_{wp}	water content at the wilting point [m^3/m^3]
F_{oc}	fraction of organic carbon [-]

Compound specific

μ_r	reference degradation rate constant [L/Kg]
DT_{50s}	half-life of the pesticide in soil [d]
K_{oc}	soil organic carbon-water partitioning coefficient [-]
W_{sol}	the water solubility [mg/L]

Crop specific

a_I, b_I, c_I,	parameters for the determination of crop coverage for irrigated maize [-]
a_{RF},b_{RF},c_{RF}	parameters for the determination of crop coverage for rain fed maize [-]
C_f	correction factor accounting for enhanced evaporation from a wet canopy [-] needs to be > 1;
p	fraction of TAW that a plant can extract from the root zone without water stress [-]
RUF	root uptake factor [-]
SF	is a factor describing the proportion of the throughfall being stem flow [-]
SFA	is the area around the stem which is affected by stem flow [cells = cm]

Other parameters

MHHG	maximum horizontal hydraulic gradient [-]
MVHG	maximum vertical hydraulic gradient [-]
SED	soil evaporation depth [cm]
X	width of the 2-D area to be covered [cm]

Variables

μ	degradation rate constant [L/Kg]
AD	accumulated deficit for irrigation [mm]
$AE_{r(i)}$	actual root segment specific water uptake [mm/d]
C	actual water content of each grid cell [mm]
C_1	higher water content of two adjacent cells [mm]
C_2	lower water content of two adjacent cells [mm]
D_r	root depletion [mm]
E_c	potential plant evapotranspiration [mm/d]
E_{cc}	potential transpiration from the dry canopy [mm/d]
E_{cw}	wet canopy evaporation [mm/d]
E_r	potential root water uptake [mm/d]
E_s	potential soil evaporation [mm/d]
ET_a	crop specific evapotranspiration [mm/d]
FCC	fraction of the surface covered by crop canopy [m^2/m^2]
Ft	factor accounting for the temperature dependency of PPP degradation [-]
Fw	factor accounting for the water content dependency of PPP degradation [-]
HG	hydraulic gradient of a pair of cells [-]

HHG	horizontal hydraulic gradient [-]
K_c	crop coefficient [-]
K_o	water stress coefficient [-]
LAI	leaf area index [-]
N_{rs}	number of living root segments [-]
RAE_r	relative mobile water taken up by a root segment in a cell [/d]
R_c	portion of the rain which falls on the crop [mm/d]
R_m	root mass [g]
S_c	storage capacity on a crop [mm]
TAW	total available water for roots [mm]
TC	total amount of the compound in the cell [mg]
TC_r	the total amount of the compound in the root of one grid cell [mg]
TC_s	total amount of the compound sorped to the soil/organic carbon of a cell [mg]
TC_w	total amount of the compound in the water phase of a cell [mg]
TC_{wm}	total amount of the compound in the mobile water of a cell [mg]
TC_{ws}	total amount of the compound in the stationary water of a cell [mg]
TF	throughfall [mm/d]
T_{spe}	time after plant emergence [d]
VHG	vertical hydraulic gradient [-]
W_{can}	water stored on the crop [mm]

Acknowledgement

Early work on the system conceptualisation was funded through BBSRC/InnovateUK Agri-Tech Catalyst Early-Stage Feasibility project 272295.

References

Addiscott, T. M., Wagenet, R. J., 1985. Concepts of solute leaching in soils – a review of modelling approaches. Journal of Soil Science. 36, (3), 411-424.

Agatz, A., Ashauer, R., Sweeney, P., Brown C.D., 2016. Prediction of pest pressure on corn root nodes: the POPP-Corn model. Journal of Pest Science. 1-12.

Allen, R., 2003. Crop coefficients. Encyclopedia of Water Science.

Allen, R. G., Pereira, L. S., Raes, D., Smith, M., 1998. Crop evapotranspiration - Guidelines for computing crop water requirements. FAO Irrigation and drainage paper 56.

Andrieu, B., Allirand, J., Jaggard, K., 1997. Ground cover and leaf area index of maize and sugar beet crops. EDP Sciences. 17, 315-321.

Bedos, C., Genermont, S., Le Cadre, E., Garcia, L., Barriuso, E., Cellier, P., 2009. Modelling pesticide volatilization after soil application using the mechanistic model Volt'Air. Atmospheric Environment. 43, 3630-3639.

Belmans, C., Dekker, LW, Bouma, J., 1982. Obtaining soil physical field data for simulating soil moisture regimes and associated potato growth. Agricultural Water Management. 5, 319-333

Boesten, J., 1994. Simulation of bentazon leacing in sandy loam soil from Mellby (Sweden) with the PESTLA model. Journal of Environmental Science and Health Part A - Environmental Science and Engineering & Toxic and Hazardous Substance Control. 29, 1231-1253.

Brouwer, C., Prins, M., 1989. Irrigation Water Management: Irrigation Scheduling. N. R. M. a. E. Department, FAO Document Repository.

Brouwer, W. W. M., 1994. Use of simulation models for registration purposes – evaluation of pesticide leaching to groundwater in the Netherlands. Journal of Environmental Science and Health Part A - Environmental Science and Engineering & Toxic and Hazardous Substance Control. 29, 1117-1132.

Carsel, R. F., Mulkey, L. A., Lorber, M. N., Baskin, L. B., 1985. The pesticide root zone model (PRZM) – a procedure for evaluating pesticide leaching threats to groundwater. Ecological Modelling. 30, 49-69.

Fantke, P., Wieland, P., Wannaz, C., Friedrich, R., Jolliet, O., 2013. Dynamics of pesticide uptake into plants: From system functioning to parsimonious modeling. Environmental Modelling & Software. 40, 316-324.

Filipović, V., Coquet, Y., Pot, V., Houot, S., Benoit, P.,2014. Modeling the effect of soil structure on water flow and isoproturon dynamics in an agricultural field receiving repeated urban waste compost application. Science of the Total Environment. 499, 546-559.

Filipović, V., Coquet, Y., Pot, V., Houot, S., Benoit, P., 2016. Modeling water and isoproturon dynamics in a heterogeneous soil profile under different urban waste compost applications. Geoderma. 268, 29-40.

FOCUS (2000). FOCUS groundwater scenarios in the EU review of active substances. Report of the FOCUS Groundwater Scenarios Workgroup. Brussel, Belgium, Health & Consumer Protection Diretorated-General rev.2: 202.

Gärdenäs, A. I., Simunek, J., Jarvis, N., van Genuchten, M. T., 2006. Two-dimensional modelling of preferential water flow and pesticide transport from a tile-drained field. Journal of Hydrology. 329, 647-660.

Garratt, J. A., Wilkins, R. M., 1999. A new approach to 2-dimensional modelling of pesticide transport in soil.

Ha, W., Mansell, R.S., Shinde, D., Kim, N.H., Ajwa, H.A., Stanley, C.D., 2009a. 2-D Simulation of Non-isothermal Fate and Transport of a Drip-applied Fumigant in Plastic-

mulched Soil Beds. I. Model Development and Performance Investigation. Transport in Porous Media. 78, 77-99.
Ha, W., Stanley, C.D., Mansell, R.S., Ajwa, H.A., 2009b. 2-D Simulation of Non-Isothermal Fate and Transport of a Drip-Applied Fumigant in Plastic-Mulched Soil Beds. II. Sensitivity Analysis and Model Application. Transport in Porous Media. 76, 431-448.
Hantush, M. M., Marino, M. A., Islam, M. R., 2000. Models for leaching of pesticides in soils and groundwater. Journal of Hydrology. 227, 66-83.
Hartmann, A., Šimůnek, J., 2015. HYDRUS Root growth module, version 1. Hydrus Software Series 5, Department of Environmental Sciences, University of California Riverside, Riverside, Ca, p.35.
Hollinger, S. E., Angel, J. R., 2009. Weather and Crops. Illinois Agronomy Handbook, University of Illinois at Urbana-Champaign, College of Agriculture, Cooperative Extension Service. 1-12.
Hutson, J.L., Wagenet, R.J., 1995. A Multiregion Model Describing Water-Flow and Solute Transport in Heterogeneous Soils. Soil Science Society of America Journal. 59, 743-751.
Illinois Climate Network (2016). Water and Atmospheric Resources Monitoring Program Griffith Drive, Champaign, IL 61820-7495, Illinois State Water Survey.
Jarvis, N. J., Hollis, J. M., Nicholls, P. H., Mayr, T., Evans, S. P., 1997. MACRO-DB: a decision-support tool for assessing pesticide fate and mobility in soils. Environmental Modelling & Software. 12, 251-265.
Jarvis, N., Larsbo, M., 2012. MACRO (v5.2): model use, calibration and validation. Transactions of the Asabe. 55, 1413-1423.
Klein, M., 1991. PELMO: Pesticide Leaching Model. Fraunhofer-Institut für Umweltchemie und Ökotoxikogie, D57392 Schmallenberg.
Kohne, J. M., Kohne, S., Simunek, J., 2009. A review of model applications for structured soils: b) Pesticide transport. Journal of Contaminant Hydrology. 104, 36-60.
Luo, L.F., Yates, S.R., Ashworth, D.J., 2011. Predicting Methyl Iodide Emission, Soil Concentration, and Pest Control in a Two-Dimensional Chamber System. Journal of Environmental Quality. 40, 109-117.
McCully, M. E., 1999. Roots in soil: Unearthing the complexities of roots and their rhizospheres. Annual Review of Plant Physiology and Plant Molecular Biology. 50, 695-+.
Nguy-Robertson, A., Gitelson, A., Peng, Y., Vina, A., Arkebauer, T., Rundquist, D., 2012. Green Leaf Area Index Estimation in Maize and Soybean: Combining Vegetation Indices to Achieve Maximal Sensitivity. AGRONOMY JOURNAL. 104, 1336-1347.
Norman, J. M., Campbell, g., 1983. Application of a Plant-Environment Model to Problems in Irrigation. Advances in Irrigation. H. Daniel, Elsevier. 2, 155-188.
Paltineanu, I., Starr ,J., 2000. Preferential water flow through corn canopy and soil water dynamics across rows. Soil Science Society of America journal. 64, 44-54.
PPDB Database University of Hertfordshire . 2013. The Pesticide Properties DataBase (PPDB) developed by the Agriculture & Environment Research Unit (AERU), University of Hertfordshire, 2006 - 2013.
Renaud, F. G., Bellamy, P. H., Brown, C. D., 2008. Simulating pesticides in ditches to assess ecological risk (SPIDER): I. Model description. Science of The Total Environment. 394, 112-123.
Šimůnek, J., Jacques, D., Langergraber, G., Bradford, S.A., Sejna, M., van Genuchten, M.T., 2013. Numerical Modeling of Contaminant Transport Using HYDRUS and its Specialized Modules. Journal of the Indian Institute of Science. 93, 265-284.
Singh, P., Kanwar, R. S., 1995. Modification of RZWQM for simulating subsurface drainage by adding a tile flow component. Transactions of the Asae. 38, 489-498.

Suarez, F., Guzman, E., Munoz, J. E., Bachmann, J., Ortiz, C., Alister, C., Kogan, M., 2013. Simazine transport in undisturbed soils from a vineyard at the Casablanca valley, Chile. Journal of Environmental Management. 117, 32-41.

Tiktak, A., de Nie, D., van der Linden, T., Kruijne, R., 2002. Modelling the leaching and drainage of pesticides in the Netherlands: the GeoPEARL model. Agronomie. 22, 373-387.

Wilensky, U., 1999. NetLogo, Center for Connected Learning and Computer-Based Modeling, Northwestern University, Evanston, IL, USA.

Zhu, Y., Shi, L.S., Yang, J.Z., Wu, J.W., Mao, D.Q., 2013. Coupling methodology and application of a fully integrated model for contaminant transport in the subsurface system. Journal of Hydrology. 501, 56-72.